

# Comparison of the identities, fluxes, and energies of ions formed in high density fluorocarbon discharges

A. N. Goyette\*, Yicheng Wang<sup>†</sup>, and J. K. Olthoff

*National Institute of Standards and Technology, Gaithersburg, MD 20899-8113 USA*

**Abstract.** Positive ion bombardment plays an essential role in plasma processing, influencing etch rates, materials selectivity and etching profiles. Experimental determination of ion identities and energies in processing plasmas provides complementary data necessary to validate the accuracy of plasma models, and contributes to a fundamental understanding of the underlying discharge physics and chemistry. We present a comparative summary of ion compositions and energy distributions in inductively coupled discharges sustained in six fluorinated compounds: CF<sub>4</sub>, CHF<sub>3</sub>, C<sub>2</sub>F<sub>6</sub>, *c*-C<sub>4</sub>F<sub>8</sub>, CF<sub>3</sub>I and CF<sub>3</sub>CH<sub>2</sub>F. Mass-resolved ion fluxes and energies are measured using a combined energy analyzer-mass spectrometer that samples ions extracted through an orifice in the lower electrode of an inductively coupled Gaseous Electronics Conference (GEC) rf reference cell. These compounds represent common plasma processing gases as well as two gases with significantly lower global warming potentials, CF<sub>3</sub>I and CF<sub>3</sub>CH<sub>2</sub>F. We compare the identities of the significant ions formed, the relative yields of CF<sub>x</sub><sup>+</sup> and secondary ions, the width and structure of the ion energy distributions, and the mean ion energies in these six plasma chemistries. The general effects of plasma operating conditions and Ar dilution on these properties are summarized.

## INTRODUCTION

Fluorinated compounds are extensively used in plasma processing applications in the microelectronics industry. Many of the fluorinated compounds used in plasma processing, however, have high global warming potentials (GWPs), and the reduction of global warming gas emissions from plasma processing is an issue of growing significance (see Table 1). One of several approaches to this problem being considered is to identify substitute plasma chemistries based upon gases having lower GWPs than those currently in use. Two such gases which have attracted particular interest are CF<sub>3</sub>I and CF<sub>3</sub>CH<sub>2</sub>F (HFC-134a). The etching properties of high density discharges sustained in each gas have been investigated in a number of recent studies [2, 3, 4, 5, 6].

The objective of this work is to present a comparative summary of ion compositions and energy distributions in inductively coupled plasmas (ICPs) sustained in six fluorinated compounds: CF<sub>4</sub>, CHF<sub>3</sub>, C<sub>2</sub>F<sub>6</sub>, *c*-C<sub>4</sub>F<sub>8</sub>, CF<sub>3</sub>I and CF<sub>3</sub>CH<sub>2</sub>F. We present mass analyzed ion energy distributions (IEDs), relative ion flux densities, and absolute total ion currents measured using a combined ion energy analyzer-mass spectrometer that

samples ions through an orifice in the lower electrode of a Gaseous Electronics Conference (GEC) rf reference cell.

## EXPERIMENT

The discharges studied were generated in a GEC rf reference cell reactor whose upper electrode has been replaced with a five-turn planar rf-induction coil behind a quartz window to produce inductively coupled discharges [7]. The design of the GEC rf reference cell is described in detail elsewhere [8, 9]. A quartz annulus developed for use in the GEC rf reference cell to allow the generation of plasmas in electronegative gases over a much broader range of pressures and powers was mounted to the upper quartz window [10]. The details of the reactor, along with the ion energy analyzer and mass spectrometer can be found in Refs. [10, 11, 12]. Mass flow controllers regulated the gas flow, which was maintained at either 3.73 μmol/s (5 sccm) for undiluted fluorocarbon gases discharges or 7.45 μmol/s (10 sccm) for mixtures of the fluorocarbon gases with Ar.

Past experience with the ion energy analyzer indicates that the ion transmission is nearly constant over the energy ranges observed here [13]. A mass-dependent transmission correction factor, however, was applied to the highest mass ions (mass > 40 u) in order to com-

---

\* Email address: goyette@eeel.nist.gov

† Email address: wang@eeel.nist.gov

**Table 1.** Atmospheric lifetimes and 100 yr global warming potentials (GWPs) of the fluorocarbon gases studied.

	Atmospheric lifetime (yr)	GWP <sub>100</sub>	Ref.
CF <sub>4</sub>	50 000	6300	[1]
C <sub>2</sub> F <sub>6</sub>	10 000	12 500	[1]
<i>c</i> -C <sub>4</sub> F <sub>8</sub>	3200	9100	[1]
CHF <sub>3</sub>	250	12 100	[1]
CF <sub>3</sub> I	$<5 \times 10^{-3}$	$<1$	[2]
CF <sub>3</sub> CH <sub>2</sub> F	14	1300	[1]

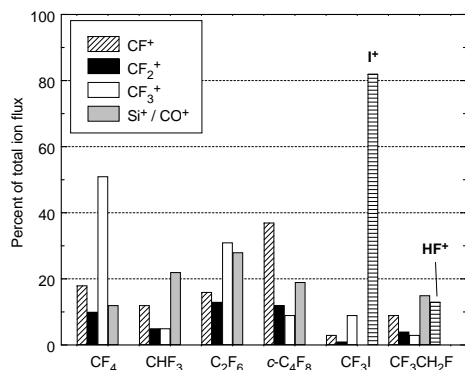


**FIGURE 1.** Relative abundances of CF<sub>x</sub><sup>+</sup> (x=1,2,3) and other significant ions (> 10% of total ion yield) detected in discharges in various fluorocarbon gases at 200 W, 1.33 Pa (10mTorr).

pensate for some decrease in the ion transmission of the quadrupole mass spectrometer with increasing mass. These factors were determined by calibration with rare gas plasmas [14] and approach a factor of 22 for I<sup>+</sup> at 127 u. For total ion current measurements, (i.e. all ion current passing through the sampling orifice), the ion optic elements at the front of the ion energy analyzer are biased such that the current passing through the sampling orifice is collected on the extractor element (the first ion optic element behind the electrode surface), and is measured using an electrometer.

The total ion current is partitioned into mass channels according to the mass spectrum of ions. The absolute intensities of the measured IEDs are then determined by scaling the measured values of the ion current for the appropriate mass channel to the total ion current. The ion flux densities presented here are derived by dividing the total measured ion current by the area of the 10 μm diameter sampling hole.

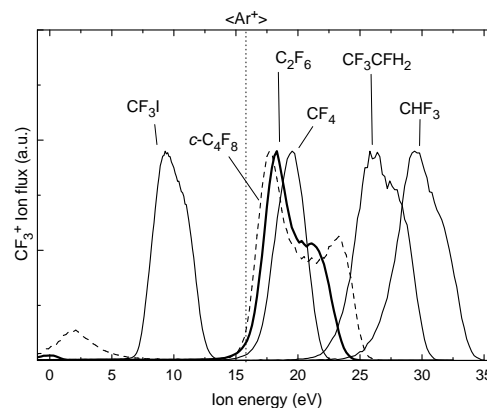
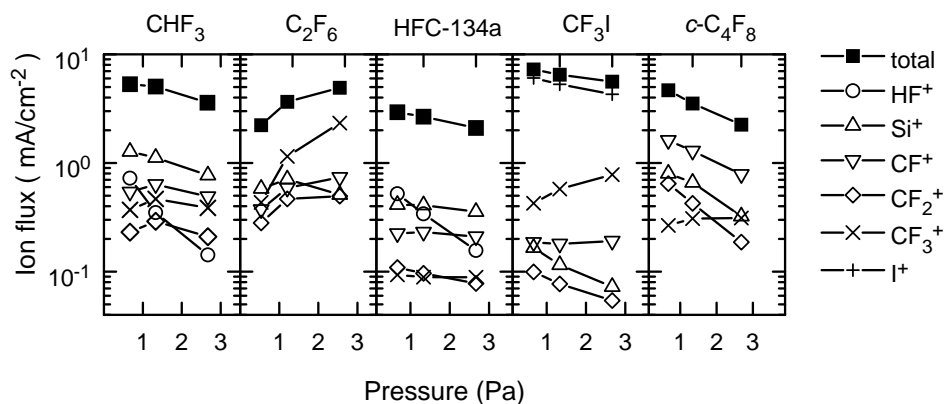


**FIGURE 2.** CF<sub>3</sub><sup>+</sup> IEDs for 1.33 Pa (10 mTorr), 200 W plasmas sustained in the six fluorocarbon gases studied. IEDs have been normalized to the same peak intensity in order to facilitate comparison. The vertical dotted line corresponds to the mean Ar<sup>+</sup> energy in a pure Ar ICP operated under the same conditions.

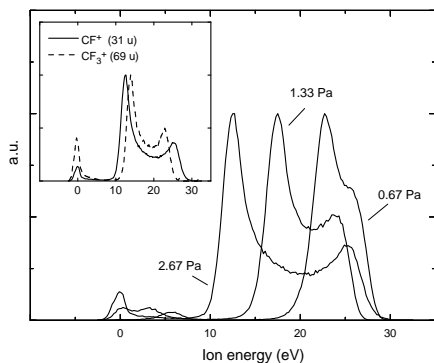
## RESULTS AND DISCUSSION

Figure 1 shows the relative abundances of CF<sub>x</sub><sup>+</sup> and other ion species comprising more than 10% of the ion current from 1.33 Pa (10 mTorr), 200 W ICPs generated in each of the fluorocarbon gases studied [10, 11, 12, 15]. In general, several ions of significant intensity were observed. In only two of the six plasma chemistries investigated did a single ionic species comprise more than half of the ion flux (CF<sub>3</sub><sup>+</sup> in CF<sub>4</sub> and I<sup>+</sup> in CF<sub>3</sub>I). Moreover, with the exception of CF<sub>3</sub><sup>+</sup> in CF<sub>4</sub> and in C<sub>2</sub>F<sub>6</sub> discharges, the dominant ion detected is not the principal ion produced by direct electron impact ionization of the feed gas. In fact, as can be seen in Fig. 1, the dominant ions detected from CHF<sub>3</sub> and HFC-134a discharges at mass 28 (the combined flux of Si<sup>+</sup> and CO<sup>+</sup> ions, which are indistinguishable in our experiments) are not produced by direct ionization of the parent gas at all, but rather as a result of plasma erosion of exposed quartz surfaces within the reactor. The absence of N<sup>+</sup> in our spectra implies N<sub>2</sub><sup>+</sup> does not contribute significantly to the 28 u ion signal. The fact that relatively small fractions of the detected ions are species which can be attributed to direct ionization of the feed gas implies considerable dissociation of the parent gas, and that ion-molecule and ion-surface interactions play significant roles in the generation and transport of ions in these plasmas. This is important from the perspective of modeling these plasmas.

The dominance of I<sup>+</sup> in CF<sub>3</sub>I discharges (typically > 80% of the total ion flux under all operating conditions investigated [15]) particularly exemplifies this.



**FIGURE 3.** Absolute ion fluxes of  $\text{CF}_x^+$  and other significant ions generated in pure fluorocarbon gases as functions of discharge pressure.



**FIGURE 4.**  $\text{CF}^+$  IEDs in  $c\text{-C}_4\text{F}_8$  ICPs as a function of pressure. Inset: Comparison of  $\text{CF}^+$  and  $\text{CF}_3^+$  IEDs in the same plasma. Note the effect of the mass of the ion on the width of the distribution.

Although the cross section for electron-impact ionization of  $\text{CF}_3\text{I}$  to form  $\text{CF}_3\text{I}^+$  is larger than the cross sections for any of the dissociative ionization channels [16], no  $\text{CF}_3\text{I}^+$  was detected from any discharge containing  $\text{CF}_3\text{I}$ . This suggests that direct electron-impact ionization of  $\text{CF}_3\text{I}$  is not a major mechanism controlling the ion composition and that a large fraction of  $\text{CF}_3\text{I}$  is dissociated in the plasma before ionization occurs. The low C-I bond energy and consequent availability of multiple dissociative mechanisms, including dissociative electron attachment, dissociative electron impact forming neutral fragments, and ultraviolet photodissociation, is likely responsible for the nearly complete dissociation of  $\text{CF}_3\text{I}$  observed in these plasmas. The rate constant for thermal dissociative electron attachment to  $\text{CF}_3\text{I}$  is  $\sim 1.7 \times 10^{-7} \text{ cm}^3 \text{ s}^{-1}$  [17]. Such high dissociative electron attachment rates likely contribute considerably to  $\text{CF}_3\text{I}$  dissociation in these discharges [6].

Figure 2 shows normalized energy distributions of  $\text{CF}_3^+$  ions obtained under the same conditions as the data in Fig. 1 [10, 11, 12, 15]. The  $\text{CF}_3^+$  IEDs vary from fairly

narrow and single-peaked for  $\text{CF}_4$  discharges to exhibiting varying degrees of broadening and bimodal splitting indicative of increased rf modulation of the ions' energy as they are accelerated across the plasma sheath. The *c*- $\text{C}_4\text{F}_8$  discharges exhibit the most pronounced bimodality. This structure in the IEDs likely results from electron attachment lowering the ground sheath capacitance. A small peak is also present near 0 eV in the  $\text{CF}_3^+$  and to a smaller extent  $\text{CF}^+$  energy distributions for some of the gases. This peak does not appear in the IEDs of the other ion species. The fact that this low-energy peak appears only for specific ion species implies that an ion dependent process such as charge exchange production of slow ions near the sampling orifice is responsible.

The mean energies of the ions which correspond to the average plasma potentials vary from 10 eV to 30 eV in these discharges under identical operating conditions. Average plasma potentials in all discharges except those generated in  $\text{CF}_3\text{I}$  are higher than those observed in pure Ar discharges operated under the same operating conditions. The nearly complete dissociation of  $\text{CF}_3\text{I}$  in the plasma, coupled with the low ionization potentials of the dissociation fragments I and  $\text{CF}_3$ , makes it likely that electron temperatures, and hence the plasma potentials, are significantly lower in  $\text{CF}_3\text{I}$  plasmas.

The influence of gas pressure on ion fluxes is shown in Fig. 3 [10, 12, 15]. The  $\text{CF}_3^+$  flux rises dramatically as a function of pressure in pure  $\text{C}_2\text{F}_6$  discharges, and to a lesser extent in pure  $\text{CF}_3\text{I}$  discharges, contributing to an overall increase in ion current under these circumstances. For all other discharges studied, the  $\text{CF}_3^+$  flux displays a much weaker dependence on discharge pressure, and the total ion flux decreases at elevated pressures.

An example of the general effect of discharge pressure on IEDs in these discharges is shown in Fig. 4 for an ICP in *c*- $\text{C}_4\text{F}_8$  [12]. The average plasma potentials in Fig. 4 decrease at higher pressures, probably due to lower mean electron energies due to higher collisional frequencies. This effect was also observed in varying degrees in the other fluorocarbon gases studied. The increase in rf sheath modulation as the pressure increases can be ascribed to a more confined plasma lowering the ground sheath capacitance. The extent to which the IEDs are broadened depends not only on the parent gas, but also upon the mass of the particular ion, with the lightest ions the most affected by the rf modulation of plasma potential. The appearance of mass-dependent structure in the energy distributions (inset of Fig. 4) illustrates the importance of measuring IEDs when determining relative ion flux intensities with the type of instrument used in this study. Under conditions such as ours, relative ion intensity measurements that utilize

simple mass scans will be affected by the energy setting of the energy analyzer. The measuring and integrating of IEDs is critical in determining accurate relative ion flux intensities.

The influence of discharge power on ion fluxes and IEDs was similarly investigated. Higher discharge powers were observed to lead to increased dissociation of the parent gas in some cases, particularly in HFC-134a discharges [15], and to shift the reactive ion composition towards higher fluxes of lighter ions. Average plasma potentials remained unaffected by discharge power, indicating that discharge power does not affect the mean energies of electrons, although significantly broadened IEDs were observed for lower discharge powers (similar to the IEDs observed at elevated pressures).

The influence of Ar dilution on ion identities and fluxes is shown in Fig. 5 [10, 11, 12, 15]. For discharges sustained in each of the fluorocarbon gases studied, the total ion flux decreases as the fluorocarbon gas is added to a pure Ar discharge and continues to do so as the concentration of the fluorocarbon gas in the feed gas mixture is raised further. This general decrease can be attributed to decreasing plasma density due to increased electron attachment with the introduction of electronegative gases. Although the  $\text{Ar}^+$  flux consistently displays a strong dependence on the Ar fraction in the feed gas mixture, the fluxes of other ion species in discharges sustained in Ar-fluorocarbon mixtures generally exhibit weaker correlations with the fluorocarbon concentration. This indicates that increased use of the reactant feed gas does not necessarily result in a corresponding increase in reactive ion flux to the surface.

## SUMMARY

We have presented a comparative summary of ion compositions and energy distributions produced in high density discharges sustained in six fluorinated compounds:  $\text{CF}_4$ ,  $\text{CHF}_3$ ,  $\text{C}_2\text{F}_6$ , *c*- $\text{C}_4\text{F}_8$ ,  $\text{CF}_3\text{I}$  and  $\text{CF}_3\text{CH}_2\text{F}$ . Several ionic species with significant fluxes were detected from these discharges, including considerable fluxes of ions resulting from erosion of exposed quartz surfaces within the reactor, particularly with the hydrofluorocarbon gases. With the exception of  $\text{CF}_3^+$  in  $\text{CF}_4$  and  $\text{C}_2\text{F}_6$  discharges, the dominant ion is not the principal ion resulting from electron-impact ionization of the feed gas. The fact that relatively small fractions of the detected ions are species which can be attributed to direct ionization of the feed gas illustrates the significance of ion-molecule and ion-surface interactions in the generation and transport of ions in these plasmas. Dissociative mechanisms also play significant roles in

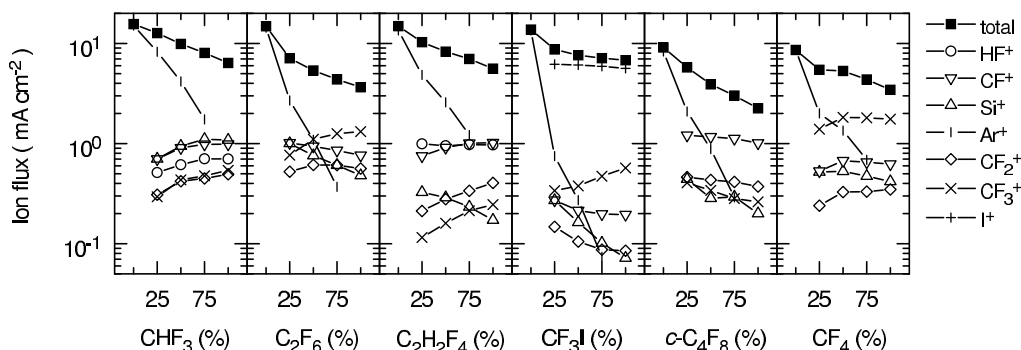


**FIGURE 5.** Absolute ion fluxes of  $\text{CF}_x^+$  and other significant ions generated in mixtures of the fluorocarbon gases and Ar as functions of the fluorocarbon concentration (by volume).

determining the identities of ions in these plasmas, particularly in  $\text{CF}_3\text{I}$  discharges in which high rates of dissociative electron attachment contribute to nearly complete dissociation of  $\text{CF}_3\text{I}$  in these discharges.

Higher discharge powers were observed to lead to increased dissociation of the parent gas in some gases, particularly in HFC-134a discharges, and shift the reactive ion composition towards higher fluxes of lighter ions. Although the  $\text{Ar}^+$  flux consistently displays a strong dependence on the Ar fraction in the feed gas mixture, the fluxes of other ion species in discharges sustained in Ar-fluorocarbon mixtures generally exhibit weaker correlations with the fluorocarbon concentration. This indicates that increased use of the reactant feed gas does not necessarily result in a corresponding increase in reactive ion flux to the surface.

Depending on the discharge conditions, the ion energy distributions vary from fairly narrow and single-peaked to very broad and bimodally structured, the latter being indicative of parasitic capacitive coupling modulating the ions' energy as they traverse the plasma

sheath. The IEDs occurring in pure  $c\text{-C}_4\text{F}_8$  discharges exhibit the most pronounced broadening and bimodality, presumably due to high rates of electron attachment lowering the ground sheath capacitance. Elevated gas pressures, lower discharge powers, and higher percentages of fluorocarbon supplied to the discharge were all observed to result in comparatively broader and more highly bimodal IEDs.

## REFERENCES

1. Houghton, J. T., Meira Filho, L. G., Bruce, J., Lee, H., Callander, B. A., Haites, E., Harris, N., and Maskell, K., eds., *Climate change, 1994 : radiative forcing of climate change and an evaluation of the IPCC IS92 emission scenarios*, New York: Cambridge University Press, 1995.
2. Karecki, S., Pruette, L., Reif, R., Sparks, T., Beu, L., and Vartanian, V., *J. Electrochem. Soc.* **145**, (1998) 4305–4312.

3. Kirmse, K. H. R., Wendt, A. E., Disch, S. B., Wu, J. Z., Abraham, I. C., Meyer, J. A., Breun, R. A., and Woods, R. C., *J. Vac. Sci. Technol. B* **14**, (1996) 710–715.
4. Misra, A., Sees, J., Hall, L., Levy, R. A., Zaitsev, V. B., Aryusook, K., Ravidranath, C., Sigal, V., Kesari, S., and Rufin, D., *Mater. Lett.* **34**, (1998) 415–419.
5. Samukawa, S., and Mukai, T., *J. Vac. Sci. Technol. B* **18**, (2000) 166–171.
6. Samukawa, S., Mukai, T., and Tsuda, K., *J. Vac. Sci. Technol. A* **17**, (1999) 1–6.
7. Miller, P. A., Hebner, G. A., Greenberg, K. E., Pochan, P. S., and Aragon, B. P., *J. Res. Natl. Inst. Stand. Technol.* **100**, (1995) 427–439.
8. Hargis, P. J., *et al.*, *Rev. Sci. Instrum.* **65**, (1994) 140–154.
9. Olthoff, J. K., and Greenberg, K. E., *J. Res. Natl. Inst. Stand. Technol.* **100**, (1995) 327–339.
10. Wang, Y., Misakian, M., Goyette, A. N., and Olthoff, J. K., *J. Appl. Phys.* Submitted.
11. Olthoff, J. K., and Wang, Y., *J. Vac. Sci. Technol. A* **17**, (1999) 1552–1555.
12. Goyette, A. N., Wang, Y., Misakian, M., and Olthoff, J. K., *J. Vac. Sci. Technol. A* In press.
13. Rao, M. V. V. S., Van Brunt, R. J., and Olthoff, J. K., *Phys. Rev. E* **54**, (1996) 5641–5656.
14. Wang, Y., and Olthoff, J. K., *J. Appl. Phys.* **85**, (1999) 6358–6365.
15. Goyette, A. N., Wang, Y., and Olthoff, J. K., *J. Phys. D* In press.
16. Olthoff, J. K., and Christophorou, L. G., *J. Phys. Chem. Ref. Data* In press.
17. Shimamori, H., and Nakatani, Y., *Chem. Phys. Lett.* **150**, (1988) 109–112.